Quantum Number Constraints from Shell Structure Govern Short-range Nucleon Pairing

D. Nguyen[1,2†], C. Yero[3,4†], H. Szumila-Vance[1,5], F. Hauenstein[1], N. Swan[3], L.B. Weinstein[3⋆], J. Kahlbow[6,7,8], G.A. Miller[9], A. Schmidt[10], E. Piasetzky[7], O. Hen[6], C. Ayerbe Gayoso[11,3], E. Cohen[7,12], P. Datta[15], A. Denniston[6], B.R. Devkota[13], M. Diefenthaler[1], C. Fogler[3], B.R. Gamage[1], D. Higinbotham[1], I. Korover[7], C. Morean[2], M. Nycz[14], M. Satnik[11], S. Seeds[15] P. Sharp[10], M. Suresh[16], A.S. Tadepalli[1], R. Wagner[7], E. W. Wertz[11]

[1]Thomas Jefferson National Accelerator Facility, Newport News, Virginia 23606, USA

[2]University of Tennessee, Knoxville, TN 37919, USA

[3]Old Dominion University, Norfolk, Virginia 23529, USA

[4]The Catholic University of America, Washington, DC 20064, USA

[5]Florida International University, Miami, FL 33199, USA

[6]Massachusetts Institute of Technology, Cambridge, Massachusetts 02139, USA

[7]School of Physics and Astronomy, Tel Aviv University, Tel Aviv 69978, Israel

[8]Lawrence Berkeley National Laboratory, Berkeley, California 94720, USA

[9]University of Washington, Seattle, WA 98195, USA

[10]The George Washington University, Washington DC 20052, USA

[11]The College of William & Mary, Williamsburg, Virginia 23185, USA

[12]Nuclear Research Center, Negev, Beer-Sheva, Israel 84190

[13]Mississippi State University, Mississippi State, Mississippi 39762, USA

[14]University of Virginia, Charlottesville, Virginia 22903, USA

[15]University of Connecticut, Storrs, Connecticut 06269, USA

[16]Hampton University, Hampton, Virginia 23669, USA

⋆Corresponding author. Email: weinstein@odu.edu

†These authors contributed equally to this work.

Atomic nuclei are intricate quantum systems in which protons and neutrons are held together by the strong nuclear force. At very short distances, nucleons can momentarily form high-momentum pairs—known as short-range correlations (SRCs)—that shape the high-momentum structure of nuclear matter. Understanding how such pairs form provides a rare experimental window into the short-range behavior of the strong interaction, with implications ranging from the structure of the atomic nucleus to the properties of neutron stars. Although many SRC properties have been investigated, the mechanism by which nucleons form SRC pairs remains poorly understood. Here we use high-energy electron scattering from a selective set of nuclei—^{40}Ca, ^{48}Ca, and ^{54}Fe—chosen for their distinct shell structures, to probe the mechanism of SRC formation. We find that SRC pairing depends far more on the specific quantum orbitals occupied by protons and neutrons than on nuclear mass or neutron–proton imbalance. Our result points to new angular-momentum quantum selection rules governing SRC pairing. This reveals a deep connection between long-range nuclear structure and short-range interactions, relevant to dense nuclear matter such as that found in neutron stars.

While atomic nuclei are complex many-body systems, they are often approximated as nucleons (protons and neutrons) moving independently within shell-model orbitals generated by a mean-field potential. Yet, the complex nature of the nucleon-nucleon force leads to the formation of temporary correlated states that go beyond the mean-field description, including short-range correlated (SRC) pairs (*1*): tightly-bound, predominantly proton-neutron pairs with high relative momentum and large

local density. These pairs dominate the high-momentum tail of the nuclear momentum distribution and account for much of the nucleons' kinetic energy (*1–9*).

Understanding SRC pair formation is crucial for describing the short-range structure of nuclei and for modeling systems with densities exceeding nuclear saturation, such as neutron stars (*10, 11*). While SRC pairs have been studied across a range of nuclei, the specific mechanisms driving their formation remain uncertain.

Here we measured the electron-induced knockout of high initial-momentum protons from ^{40}Ca, ^{48}Ca, and ^{54}Fe, see Fig. 1. ^{40}Ca and ^{48}Ca are both doubly magic (closed shell), with the latter containing eight (40%) more neutrons in the $1f_{7/2}$ orbital. ^{54}Fe adds six more protons to the $1f_{7/2}$ orbital, resulting in an almost symmetric, almost doubly-magic nucleus, much like ^{40}Ca, but 35% heavier. Therefore by comparing the asymmetric ^{48}Ca to the lighter ^{40}Ca and the heavier ^{54}Fe, we can better understand the roles of the different possible pair-formation mechanisms.

Surprisingly, we find almost no enhancement in the number of protons knocked out from SRC pairs in ^{48}Ca. However, the additional six $1f_{7/2}$ protons of ^{54}Fe, lead to ~50% more protons in SRC pairs. These results challenge the expectation that SRC pair formation scales simply with either mass or neutron excess (*4*). Instead, they suggest that nucleons preferentially form SRC pairs with partners occupying the same orbital, where spatial overlap and angular momentum alignment are maximal.

Background

Electron scattering experiments at large momentum transfer ($Q^2 \geq 1.5$ GeV$^2/c^2$) and large Bjorken-x ($x_B = Q^2/2m\omega \geq 1.2$, where m is the nucleon mass and ω is the energy transfer) have found that short-range correlated nucleon pairs are predominantly proton-neutron pairs, are found in all nuclei, and account for almost all of the high-momentum nucleons (above the Fermi momentum) (*1, 2*).

On the theoretical side, significant progress has been made in describing SRC pairs from first principles. Many-body numerical calculations provide position and momentum space densities for a range of light to medium mass nuclei (*12, 13*), showcasing the universal nature of SRC pairs. Effective field theory techniques utilized scale separation and factorization to show that the dynamics of the nucleons within the pair is a short-distance phenomenon while pair formation is a

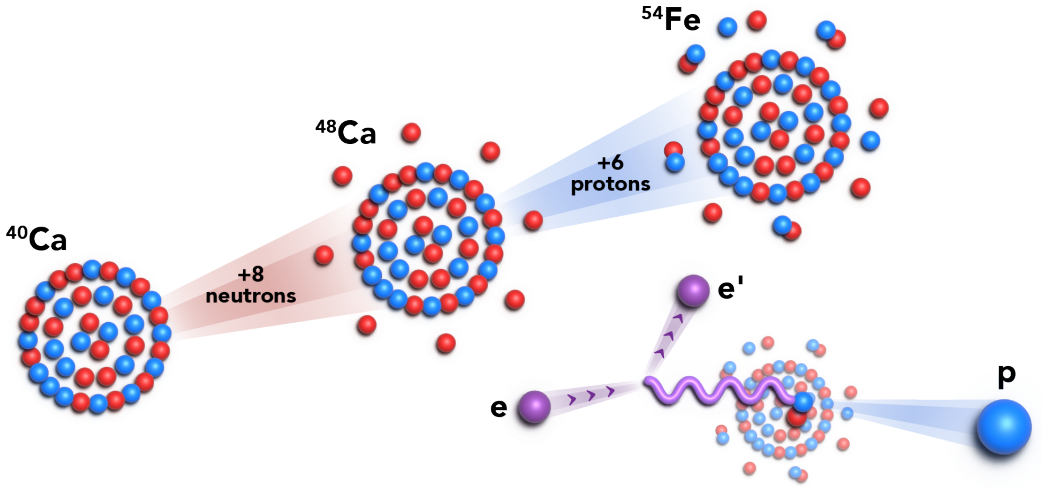

Figure 1: **Schematic representation of orbital structure of the "CaFe" nuclei.** ^{40}Ca with 20 (blue) protons and 20 (red) neutrons in the $1s$, $1p$, and $2s$, $1d$ orbitals, ^{48}Ca with eight more $1f_{7/2}$ neutrons, and ^{54}Fe with six more $1f_{7/2}$ protons. The lower right shows a schematic of the reaction, with an electron (purple) scattering from a nucleus by emitting a (purple) virtual photon which knocks out a proton (blue) from an np correlated pair in a nucleus.

long-range phenomenon sensitive to nuclear-structure details (*14–16*).

Therefore, a comprehensive understanding of SRC pairs requires understanding pair-formation mechanisms, i.e., how SRC pairing changes with nuclear mass and neutron excess. Duer *et al.* (*4*), studied this by comparing proton and neutron knockout from a range of nuclei (^{12}C, ^{27}Al, ^{56}Fe, ^{208}Pb) with varying mass and neutron excess. They found an increased proton pairing probability in nuclei with a greater neutron excess. These extra high-momentum protons suggested that the excess neutrons in asymmetric nuclei form additional np SRC pairs. However, since both mass and neutron excess increased together in the four measured nuclei, the data could not separate their contributions.

A previous inclusive-scattering measurement tried to address this by comparing ^{40}Ca and ^{48}Ca. Their results suggested a 17% increase in SRC pair formation due to the 40% increase in neutrons (*17*). However, a follow-up analysis found that due to the inclusive nature of the measurement, significant model-interpretation uncertainties are possible (*18*).

Results

We measured the probability of proton knockout from SRC pairs by scattering 10.5-GeV electrons from ^{40}Ca, ^{48}Ca, and ^{54}Fe targets in Jefferson Lab's Hall C. The experiment, conducted in 2023, used the Super High Momentum Spectrometer (SHMS) (*19*) to detect scattered electrons at a central scattering angle of $\theta_e = 8.3°$ and a central momentum of 8.55 GeV/c, and the High Momentum Spectrometer (HMS) (*20*) to detect knocked-out protons at a central scattering angle of $\theta_p = 66.4°$ and a central momentum of 1.325 GeV/c. These small-aperture magnetic spectrometers determine particle momenta by tracking curvature in the magnetic field. See Supplemental Material (*21*) for details.

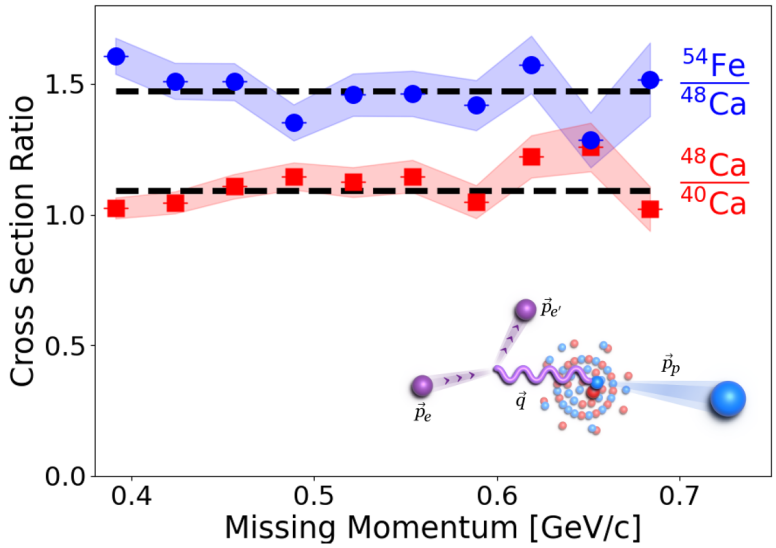

Figure 2: **The per-nucleus $(e, e'p)$ cross-section ratios for ^{48}Ca/^{40}Ca (red squares) and ^{54}Fe/^{48}Ca (blue circles) plotted versus missing momentum** p_{miss}. The dashed lines show the weighted averages of data points. The corresponding χ^2/dof of the fits are 1.46 (^{48}Ca/^{40}Ca) and 1.32 (^{54}Fe/^{48}Ca). The inset shows the electron scattering from a nucleus, knocking out a proton from an SRC pair. The initial and scattered electron momenta are $\vec{p}_e$ and $\vec{p}_{e'}$, the transferred momentum is $\vec{q}$ and the outgoing proton momentum is $\vec{p}_p$. The missing momentum $p_{miss} = |\vec{p}_p - \vec{q}\,|$.

To select events dominated by proton knockout from SRC pairs, we required a squared momentum transfer $Q^2 \geq 1.8$ GeV$^2/c^2$, Bjorken scaling variable $x_{bj} \geq 1.2$, missing momentum

$0.375 \leq p_{miss} \leq 0.700$ GeV/c, and the angle between the recoil nucleus and the momentum transfer, $\theta_{rq} \leq 40^{\circ}$. These kinematic cuts isolate quasielastic scattering from high-initial-momentum nucleons, which are predominantly members of SRC pairs (*8*). They also reduce the effects of final-state rescattering. The missing momentum, $p_{miss} = |\vec{p} - \vec{q}\,|$, corresponds approximately to the initial momentum of the struck nucleon and was calculated from the difference between the measured knocked-out proton momentum and the momentum transfer.

We extracted cross sections as a function of p_{miss} for each nucleus, integrated over the detector acceptances. From these, we computed cross-section ratios, which provide a relative measure of SRC-pair probabilities. Since the calculated momentum distributions of SRC pairs are almost identical in all nuclei (to within an overall scale factor), the ratios of ^{48}Ca to ^{40}Ca and ^{54}Fe to ^{48}Ca should be constant across the measured p_{miss} range. The constancy of our data with p_{miss} (Fig. 2) validates that we are measuring proton knockout from SRC pairs. We then compared the integrated per-nucleus cross-section ratios (Fig. 3) and found that the SRC proton-knockout ratio in ^{48}Ca is 1.10 ± 0.02 times that of ^{40}Ca. This is slightly lower than, though consistent within uncertainties, the measured inclusive ratio of 1.165 ± 0.014 (*17*). In contrast, the ratio of ^{54}Fe to ^{48}Ca is much larger, 1.49 ± 0.03, indicating a substantially higher probability of SRC proton knockout in ^{54}Fe.

This pattern reveals a striking asymmetry. Increasing the neutron number by 40% from ^{40}Ca to ^{48}Ca leads to only a ~10% increase in SRC proton probability. However, adding six more protons from ^{48}Ca to ^{54}Fe results in a ~50% increase. These findings suggest that the eight $1f_{7/2}$ neutrons in ^{48}Ca do not efficiently form SRC pairs with inner-orbital protons. In contrast, the added six $1f_{7/2}$ protons in ^{54}Fe pair strongly with the $1f_{7/2}$ neutrons, likely due to increased spatial overlap and favorable quantum numbers. A schematic summary of the inferred intra- and inter-orbital pairing strengths is shown in the Fig. 3 inset. These results underscore the importance of orbital structure in driving SRC pair formation and provide new experimental constraints for models of dense nuclear matter.

We compared our results to different models (see Fig. 3). Ryckebusch *et al.* (*16*) used the low-order correlation operator approximation (LCA) to compute the SRC contribution to the single-nucleon momentum distribution. Tropiano *et al.* (*22*) computed SRC-pair-sensitive momentum distributions using similarity renormalization group (SRG)-evolved operators and empirically tuned single-particle wave functions. The relative fractions of high-momentum protons should ap-

proximately equal the relative SRC-pair abundances. Both momentum distribution ratios slightly overestimated the ^{48}Ca/^{40}Ca ratio and dramatically underestimated the ^{54}Fe/^{48}Ca ratio.

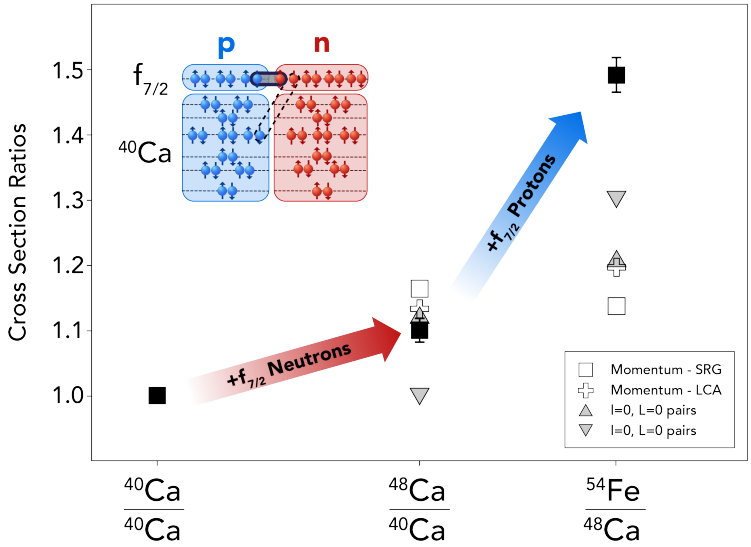

Figure 3: **The per-nucleus integrated** $(e, e'p)$ **cross-section ratios for** ^{40}**Ca/**^{40}**Ca,** ^{48}**Ca/**^{40}**Ca, and** ^{54}**Fe/**^{48}**Ca.** The filled black squares show the data, the open squares show the SRG-based momentum-distribution model (*22*), the open '+' signs show the LCA-based momentum distribution (*16*), the gray triangles show quantum pairing calculations of (upright triangles) the Colle (*23*) $l = 0, n = 0$ quantum-pairing model, and (inverted triangles) the more restrictive $L = 0, l = 0$ quantum-pairing model. The upper-left inset shows the orbital structure of ^{40}Ca, the eight additional $1f_{7/2}$ neutrons in ^{48}Ca, and the six additional $1f_{7/2}$ protons in ^{54}Fe. The dashed ellipse represents the observed weak inter-orbital pairing and the solid ellipse represents the observed strong intra-orbital pairing.

Phenomenological models based on the orbital structure of nuclei offer additional guidance. Colle *et al.* (*23*) used shell-model wave functions to estimate the relative numbers of pp and pn pairs across nuclei. They found that allowing only nodeless ($n = 0$) S-state ($l = 0$) np pairs—better matched the previous data. This quantum selection rule overestimated our ^{48}Ca/^{40}Ca ratio and significantly underestimated the ^{54}Fe/^{48}Ca ratio.

We introduced a more selective quantum-pairing model, requiring SRC pairs to have both zero relative ($l = 0$) and total ($L = 0$) angular momentum (*24*). This eliminates pairing between nucleons

in different orbitals and predicts: no increase in SRC pairs for ^{48}Ca relative to ^{40}Ca, and a ~30% increase for ^{54}Fe due to the additional $1f_{7/2}$ protons. This more restrictive model described the data better, but still underestimated the ^{54}Fe/^{48}Ca ratio.

Both of these quantum selection models neglect pp pairs, which should be at most a 10% effect in ^{54}Fe. Our model also neglects pairing between $1s$ neutrons and $2s$ protons (and vice versa), which should be about ten times smaller than $1s-1s$ and $2s-2s$ pairing, due to the mismatch in the radial distribution.

Discussion

Our results point to a key organizing principle in the formation of SRC nucleon pairs: quantum number constraints imposed by shell structure are more important than either mass or neutron excess. The eight $1f_{7/2}$ neutrons in ^{48}Ca couple weakly to the core protons. The extra six $1f_{7/2}$ protons in ^{54}Fe couple unexpectedly strongly to the eight $1f_{7/2}$ neutrons. Models based on momentum distributions fail to describe the observed ratios. Instead, models that incorporate more-restrictive quantum-mechanical selection rules on the angular momentum states of pairing nucleons more accurately describe the data.

These findings impose important new constraints on theoretical models of nuclear structure and the dynamics of dense nuclear matter. They suggest that SRC-pair formation is not only simply a universal many-body feature of the nuclear wave function, but also reflects the quantum architecture of the nucleus itself. By demonstrating that angular momentum selection rules shape the SRC-pair landscape, this work opens new pathways for exploring the interplay between mean-field structure and short-range dynamics in nuclei.

These insights are important for modeling the structure of neutron-rich matter in extreme environments, including neutron stars, where SRC pairs influence the equation of state, neutrino opacities, and dense-matter response. Ultimately, bridging mean-field structure and short-range dynamics is key to a unified description of nuclear matter from finite nuclei to astrophysical scales.

References and Notes

1. O. Hen, G. A. Miller, E. Piasetzky, L. B. Weinstein, Nucleon-Nucleon Correlations, Short-lived Excitations, and the Quarks Within. *Rev. Mod. Phys.* **89** (4), 045002 (2017), doi:10.1103/RevModPhys.89.045002.

2. E. I. Piasetzky, L. B. Weinstein, *Measurements of NN Correlations in Nuclei* (Springer Singapore), pp. 1–22 (2022), doi:10.1007/978-981-15-8818-1_60-1.

3. A. Schmidt, *et al.*, Probing the core of the strong nuclear interaction. *Nature* **578** (7796), 540–544 (2020), doi:10.1038/s41586-020-2021-6.

4. M. Duer, *et al.*, Probing high-momentum protons and neutrons in neutron-rich nuclei. *Nature* **560** (7720), 617–621 (2018), doi:10.1038/s41586-018-0400-z.

5. E. O. Cohen, *et al.*, Center of Mass Motion of Short-Range Correlated Nucleon Pairs studied via the $A(e, e'pp)$ Reaction. *Phys. Rev. Lett.* **121** (9), 092501 (2018), doi:10.1103/PhysRevLett.121.092501.

6. M. Duer, *et al.*, Direct Observation of Proton-Neutron Short-Range Correlation Dominance in Heavy Nuclei. *Phys. Rev. Lett.* **122**, 172502 (2019), doi:10.1103/PhysRevLett.122.172502.

7. I. Korover, *et al.*, 12C(e,e'pN) measurements of short range correlations in the tensor-to-scalar interaction transition region. *Phys. Lett. B* **820**, 136523 (2021), doi:10.1016/j.physletb.2021.136523.

8. I. Korover, *et al.*, Observation of large missing-momentum (e,e'p) cross-section scaling and the onset of correlated-pair dominance in nuclei. *Phys. Rev. C* **107** (6), L061301 (2023), doi:10.1103/PhysRevC.107.L061301.

9. R. Subedi, *et al.*, Probing Cold Dense Nuclear Matter. *Science* **320**, 1476–1478 (2008), doi:10.1126/science.1156675.

10. B.-A. Li, B.-J. Cai, L.-W. Chen, J. Xu, Nucleon effective masses in neutron-rich matter. *Progress in Particle and Nuclear Physics* **99**, 29–119 (2018).

11. O. Hen, B.-A. Li, W.-J. Guo, L. B. Weinstein, E. Piasetzky, Symmetry energy of nucleonic matter with tensor correlations. *Phys. Rev. C* **91**, 025803 (2015), doi:10.1103/PhysRevC.91.025803.

12. J. Carlson, S. Gandolfi, A. Gezerlis, Quantum Monte Carlo approaches to nuclear and atomic physics. *Prog. Theor. Exp. Phys.* **01A**, 209 (2012).

13. J. Carlson, *et al.*, Quantum Monte Carlo methods for nuclear physics. *Rev. Mod. Phys.* **87**, 1067 (2015), doi:10.1103/RevModPhys.87.1067.

14. R. Cruz-Torres, *et al.*, Many-Body Factorization and Position-Momentum Equivalence of Nuclear Short-Range Correlations. *Nature Physics* **17**, 306 (2020).

15. A. J. Tropiano, S. K. Bogner, R. J. Furnstahl, Short-range correlation physics at low renormalization group resolution. *Phys. Rev. C* **104** (3), 034311 (2021), doi:10.1103/PhysRevC.104.034311.

16. J. Ryckebusch, W. Cosyn, T. Vieijra, C. Casert, Isospin composition of the high-momentum fluctuations in nuclei from asymptotic momentum distributions. *Phys. Rev. C* **100** (5), 054620 (2019), doi:10.1103/PhysRevC.100.054620.

17. D. Nguyen, *et al.*, Novel observation of isospin structure of short-range correlations in calcium isotopes. *Phys. Rev. C* **102**, 064004 (2020), doi:10.1103/PhysRevC.102.064004, `https://link.aps.org/doi/10.1103/PhysRevC.102.064004`.

18. R. Weiss, *et al.*, Extracting the number of short-range correlated nucleon pairs from inclusive electron scattering data. *Phys. Rev. C* **103** (3), L031301 (2021), doi:10.1103/PhysRevC.103.L031301.

19. S. Ali, *et al.*, The SHMS 11 GeV/c Spectrometer in Hall C at Jefferson Lab. *Nucl. Inst. and Meth. A* **under review** (2025).

20. O. K. Baker, *et al.*, The High Momentum Spectrometer drift chambers in Hall C at CEBAF. *Nucl. Instrum. Meth. A* **367**, 92–95 (1995), doi:10.1016/0168-9002(95)00737-7.

21. Materials and methods are available as supplementary material.

22. A. J. Tropiano, *et al.*, High-resolution momentum distributions from low-resolution wave functions. *Phys. Lett. B* **852**, 138591 (2024), doi:10.1016/j.physletb.2024.138591.

23. C. Colle, *et al.*, Extracting the mass dependence and quantum numbers of short-range correlated pairs from $A(e,e'p)$ and $A(e,e'pp)$ scattering. *Phys. Rev. C* **92**, 024604 (2015), doi:10.1103/PhysRevC.92.024604.

24. A. Lane, *Nuclear Theory* (W.A. Benjamin, New York) (1964).

Acknowledgments

We acknowledge support from the National Science Foundation MPS-Ascend Postdoctoral Research Fellowship Grant No. 2137604, the U.S. Department of Energy, D.O.E. grants DE-SC0022007, DE-FG02-96ER40960, DOE DE-SC0013615 the Jefferson Lab Nathan Isgur Fellowship, and the United States-Israel Binational Science Foundation (BSF) grant 2018093. Jefferson Science Associates operates the Thomas Jefferson National Accelerator Facility for the DOE, Office of Science, Office of Nuclear Physics under contract DE-AC05-06OR23177. We are also grateful to all granting agencies providing funding support to the authors of this project.

We are grateful for the efforts and support of the staff of the Accelerator and Physics Divisions at Jefferson Lab that made this experiment possible.

Supplementary materials

Materials and Methods

Supplementary Text

Tables S1 to S2

Figures S1 to S6

References *(8, 24-30)*